

Quantification of collective behaviour via movement tracking

Kirill Lonhus, Dalibor Štys, & Renata Rychtáriková

¹*University of South Bohemia in České Budějovice, Faculty of Fisheries and Protection of Waters, South Bohemian Research Center of Aquaculture and Biodiversity of Hydrocenoses, Institute of Complex Systems, Zámek 136, 373 33 Nové Hrady, Czech Republic.*

Terms such as *leader*, *follower*, and *oppressed* sound equally well in the description of a pack of wolves, an insect community, a street protest crowd or a business team, and have very similar meanings. Use of these terms implies presence of some general law or structure that govern collective behaviour. We picked up the most common parameter for all levels of organization – motion. All possible manifestations were reduced to individual agents' trajectories. This allowed us to calculate windowed distance correlations and then make a causality analysis to determine who follows whom. This resulted in time-resolved graphs, which show who follows whom in a group. It characterize an observed system in a general but easy interpretable way. The theoretical findings were verified on an aquarium fish school. The observed patterns are in agreement with expected behaviour.

1 INTRODUCTION

Collective behaviour is one of the most enigmatic phenomena of contemporary times¹. It is a truly omnipresent phenomenon – from flocking behaviour of birds and growth of bacterial colonies² to stock exchange trading and school class hierarchy. We feel intuitively that something should be common – because the observed behaviour patterns and roles of agents (*leader*, *follower*, *oppressed*, *crowd*) sound applicable. This implies a presence of some general law or structure, which is common for most living species and irrelevant to a level of organization³.

The aim of this work is to justify and formalize such a general meaning, and empirically verify the findings. In order to be able to link such diverse levels of collective behaviour, one need to select its common manifestation. We selected *the motion*. This term has a similar meaning (aim) for most groups of living species (a move from "bad" to "good") and is invariant to organization level (degree of evolution). For instance, cells move from a place without nutrients to a place with nutrients or dogs run away from vehicles.

One of the most widespread approaches to motion analysis is the relative position analysis. This has been successfully applied in analysis of the human⁴ and fish⁵ behaviour. The relative position analysis has a very clear interpretation but is weakly data-driven. A researcher has to

insert *a priori* knowledge (e.g., existence of the leader or an exploring pattern) about the observed phenomenon and then fit the data to such an understanding. Another way in the motion analysis is to follow a full-model approach, considering living objects as particles driven by fixed forces and pre-defined potentials. It is the most mature but still not entirely general approach that could be applied to at least most systems³. The model-locked approach still requires *a priori* understanding of objects and, again, shows only things, which a researcher is aware of. This approach is a great tool for quantification of known phenomena, but not for discovering new ones.

Due to the lack of a model-free data-mining instrument that would be able to convert the recorded trajectories to biologically relevant parameters, we decided to invent a new tool. We selected a small aquarium fish – Tiger Barb – as the model organism. This species is very active and keen, able to form shoals from 5 individuals⁶. The complex collective behaviour is expected. In order to track movement of each individual fish without any label, video analysis was used.

2 RESULTS

Fish tracking

During the experiment, the aquarium with fish was recorded with a frequency of 25 fps. The images were stored uncompressed, in the 16-bit depth. *Prior to* further processing, the camera images had to be separated to corresponding views. The corners of the aquarium were annotated manually (total 28 points) and then fitted by a projective transformation. As the side effect, the projective transformation compensated for the distortion of the corresponding views (Figure 1) and the aspect ratio became linearly proportional to the real size of the aquarium.

The aquarium front view giving the z -coordinates of the fish localization was always processed separately. The bottom and the top view were almost the same but only mutually flipped (in terms of coordinates x, y) and, thus, were usually averaged. In case that the fish were overlapping in the top view and not in the bottom view (or vice versa), the bottom and the top view were processed separately to give better tracks.

The general method pipeline was inspired by⁷ and⁵ but rewritten from scratch. The difference is that the original algorithm is 2D, but in our case there are three 2D views that allow us the reconstruction of 3D positions (with x - y redundancy when one view is from above and the second one is from below the aquarium). This is achieved by re-projecting the coordinates and calculating the overlap of coordinates between the assembled trajectories in different views. This allows us to permute the classifiers in such a way that the first (for all views) detects the same fish in the corresponding views. In this way, we got a consistent annotation between views and then get a 3D position that is not very different from the original approach. The re-designed tracking algorithm is schematically shown in Figure 2A.

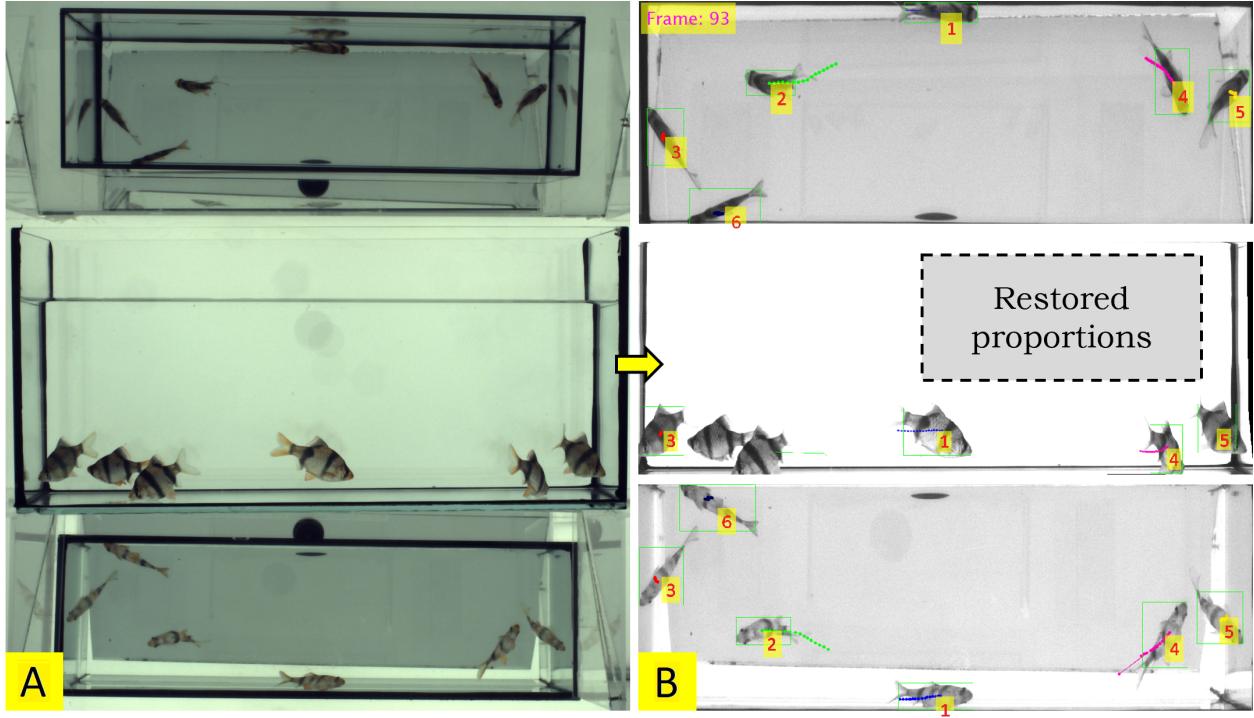


Figure 1: (A) The experimental setup (a fish aquarium with two side mirrors) and (B) tracking of individual objects (fish) in the multiple views after image geometry restoration.

In the first step, a simple foreground detection, based on median background estimation, was used. This foreground detection is very robust and showed a high recall. The detected objects were then classified as individuals/overlaps using a small VGG-like⁸ CNN. This CNN annotation was generated automatically, based on average areas and perimeters of the detected objects. The detections for each individual fish were assembled into continuous sequences – tracklets – based on the overlapping their bounding boxes in each two consecutive frames. In certain cases, it was possible to resolve the overlaps of two fish⁹ to increase the continuity of the tracklets.

The sequences of images, where the number of the detected objects coincides with the number of the fish in the experiment, were used as seeds for the next CNN-based classifier. These sequences for the different sides of the aquarium were matched using projection of coordinates and overlap in time domain in a way described in⁷ and used for training the classifier. Then, all objects were classified. Among them, trustworthy (which are in agreement) sequences were selected and used for training. Four passes were typically enough to achieve a high (0.98) classification accuracy. In the same way, the whole tracklets were classified. The tracklets from different views were projected (using known proportion between coordinates) and merged, which gave 3D coordinates in [mm].

Certain post-processing steps were applied to fill the gaps in the trajectories (where it was

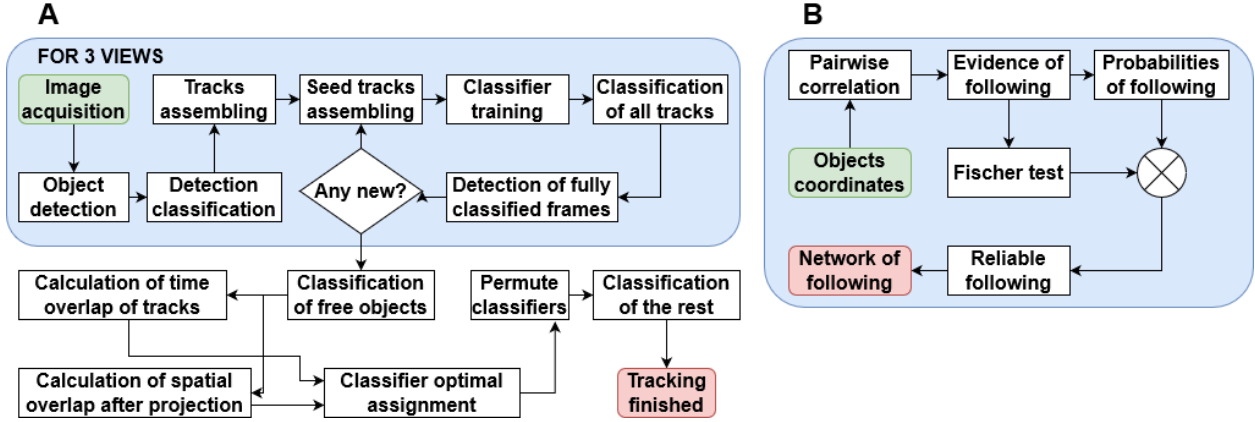


Figure 2: **(A)** Scheme of the tracking algorithm and extraction of objects' coordinates. **(B)** Scheme of the algorithm for construction of networks of following. This algorithm arises from the tracking algorithm **A**.

possible to do it unambiguously via overlap uniqueness), by a simple linear interpolation between the ends of the parts of the trajectories. The accuracy of the method was verified only visually, but the method was designed similarly to ⁷ and thus its accuracy is assumed to be comparable. Due to the design of the method, visual inspection of the fish trajectories has not shown any significant errors. The output of this step is a time-resolved 3D trajectory of each individual fish. We intentionally did not describe the tracking algorithm in depth, because the processing and analysis below are not only narrowly limited to this data but can be applied to any type of position tracking data. But the full code with comments is available in supplementary materials.

Determination of temporal correlations

To compare the results for different species/levels of organization, we needed to decouple the behaviour from the motion. For this, the distance correlation was used. The idea was simple – to rewrite the classical covariance by the multiplication of the signed distances. Let A, B be scalar sequences of length N , then

$$\text{cov}(A, B) = \frac{1}{N^2} \sum_i^N \sum_j^N (A_i - \bar{A}) \cdot (B_i - \bar{B}) = \frac{1}{N^2} \sum_i^N \sum_j^N D_{ij}(A) \cdot D_{ij}(B) \quad (1)$$

where $D_{ij}(X)$ is a signed distance between elements i and j of arbitrary sequence X . If we replace such a signed distance by the Euclidean distance $D_{ij}(\vec{X}) = \|\vec{X}_i - \vec{X}_j\|$, the obtained function will behave very similar to the classical covariance and let us denote it as a distance covariance. Such a definition allows us to introduce a Pearson-like correlation coefficient, which we denoted the

distance correlation, by replacing the covariances with the distance covariances:

$$\text{corr}(\vec{A}, \vec{B}) = N^2 \frac{\sum_{i,j} \|\vec{A}_i - \vec{A}_j\| \cdot \|\vec{B}_i - \vec{B}_j\|}{(\sum_{i,j} \|\vec{A}_i - \vec{A}_j\|^2) \cdot (\sum_{i,j} \|\vec{B}_i - \vec{B}_j\|^2)}, \quad (2)$$

where \vec{A}, \vec{B} are vector sequences with the length of $N = \{..., i, j, ...\}$ points in the Euclidean space of the same dimensionality. Despite its simplicity, this method was rigorously done and investigated quite recently¹⁰. However, it varies from $[0, 1]$ instead of $[-1, 1]$, which is a direct consequence of the presence of the unsigned distance. As shown in even more recent paper¹¹, such correlation shows most of the properties and common meaning of the ordinary correlation.

In our application, the correlation in Equation 2 was used as a measure of the trajectories' similarity in the most general sense. The correlation between positions in a sliding window for two selected objects on a timeline gave the local similarity of their motion (Figure 3A).

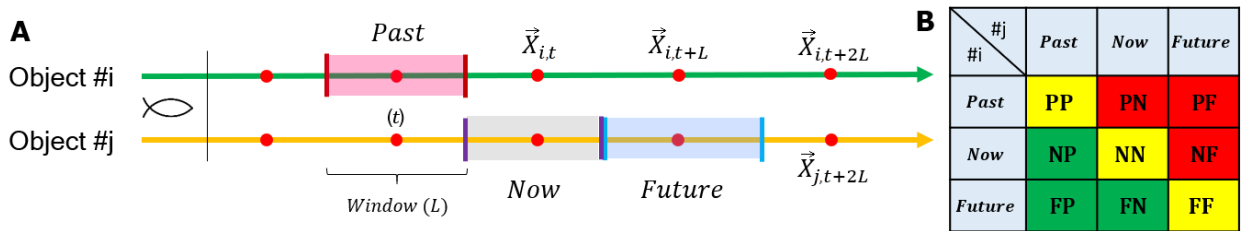


Figure 3: (A) The timelines for two objects with relevant correlation time windows of the length L . (B) The matrix shows the favorable (green), neutral (yellow), and unfavorable (red) combinations of correlations for a situation when object i follows object j . Symbols **P**, **N**, and **F** denotes the past, current, and future states of the object i or j , respectively.

It is also possible to select misaligned windows on the time arrow. For an object, let us select three dedicated time windows centered at times t , $t-L$, and $t+L$, respectively, where L is a window size, and denote them as **Past**, **Now**, and **Future**. Thus, any pair of objects has 9 combinations of two windows: one for the first object, one for the second one. Let us denote the objects' states by two-letter codes: the first object's time states, shortened to one letter, and second one. For example, **PF** means a comparison of the first object's past position with the second object's future position. This notation helped us to analyse physical interpretation and causality of such shifted correlations.

Construction of networks of following

Let us define the term *following* in this way: if object i 's *future state* correlates with object j 's *past state*, then *object i follows object j* .

If we consider the hypothesis that i follows j then combinations of time windows can be

classified into 3 groups (Figure 3B): supporting the hypothesis $S = \{\mathbf{NP}, \mathbf{FP}, \mathbf{FN}\}$, neutral to the hypothesis $N = \{\mathbf{PP}, \mathbf{NN}, \mathbf{FF}\}$, and rejecting the hypothesis $R = \{\mathbf{PN}, \mathbf{PF}, \mathbf{NF}\}$. If each time window is taken from each group always only once, it gives 3^3 combinations. We denoted as an evidence the fact that one correlation is higher than another. Such an evidence is treated as significant if the corresponding correlation is higher than the correlation from the neutral group. In the next step, we evaluated a statistical significance of the hypothesis whether the tendency that object i follows object j and vice versa is higher than that object j follows object i . For each pair of objects i and j , we have four possibilities how the objects follow each other in a time window: i follows j , j follows i , i does not follow j , j does not follow i . The whole algorithm for construction of networks of following is depicted in Figure 2B.

The total numbers of the significant evidences during the experiment are

$$e^{(i \rightarrow j)} = \sum_{s^{(i \rightarrow j)}}^{S^{(i \rightarrow j)}} \sum_n^N \sum_{r^{(i \rightarrow j)}}^{R^{(i \rightarrow j)}} [s^{(i \rightarrow j)} > n] \cdot [s^{(i \rightarrow j)} > r^{(i \rightarrow j)}], \quad (3)$$

$$e^{(j \rightarrow i)} = \sum_{s^{(j \rightarrow i)}}^{S^{(j \rightarrow i)}} \sum_n^N \sum_{r^{(j \rightarrow i)}}^{R^{(j \rightarrow i)}} [s^{(j \rightarrow i)} > n] \cdot [s^{(j \rightarrow i)} > r^{(j \rightarrow i)}], \quad (4)$$

$$e^{(i \not\rightarrow j)} = \sum_{r^{(i \not\rightarrow j)}}^{R^{(i \not\rightarrow j)}} \sum_n^N \sum_{s^{(i \not\rightarrow j)}}^{S^{(i \not\rightarrow j)}} [r^{(i \not\rightarrow j)} > n] \cdot [r^{(i \not\rightarrow j)} > s^{(i \not\rightarrow j)}], \quad (5)$$

$$e^{(j \not\rightarrow i)} = \sum_{r^{(j \not\rightarrow i)}}^{R^{(j \not\rightarrow i)}} \sum_n^N \sum_{s^{(j \not\rightarrow i)}}^{S^{(j \not\rightarrow i)}} [r^{(j \not\rightarrow i)} > n] \cdot [r^{(j \not\rightarrow i)} > s^{(j \not\rightarrow i)}], \quad (6)$$

where $e^{(i \rightarrow j)}$, $e^{(j \rightarrow i)}$, $e^{(i \not\rightarrow j)}$, and $e^{(j \not\rightarrow i)}$ are sums of significant evidences when object i follows object j , object j follows object i , object i does not follow object j , and object j does not follow object i , respectively. Variables $s^{(i \rightarrow j)}$ and $s^{(j \rightarrow i)}$ denote correlations supporting the hypothesis that object i follows object j and vice versa, respectively. The analogous variables $r^{(i \rightarrow j)}$ and $r^{(j \rightarrow i)}$ denote correlations rejecting the hypothesis that object i follows object j and vice versa, respectively. Variable $n \in N$ is a combination of time windows that is neutral to the hypothesis of following.

The discrete sums of the significant evidences (Eqs. 3–6) were firstly used as an input into the Fisher exact test ¹² to calculate the precise p -value. In this case, the meaning of the p -value is a measure of the deviation from the hypothesis that no one follows anyone. From Table 1 the p -value of the Fisher test was calculated as

$$\begin{aligned}
p &= \frac{\binom{e^{(i \rightarrow j)} + e^{(j \rightarrow i)}}{e^{(i \rightarrow j)}} \binom{e^{(i \not\rightarrow j)} + e^{(j \not\rightarrow i)}}{e^{(i \not\rightarrow j)}}}{\binom{e^{(i \rightarrow j)} + e^{(j \rightarrow i)} e^{(i \not\rightarrow j)} + e^{(j \not\rightarrow i)}}{e^{(i \rightarrow j)} + e^{(j \rightarrow i)}}} \equiv \frac{\binom{e^{(i \rightarrow j)} + e^{(j \rightarrow i)}}{e^{(j \rightarrow i)}} \binom{e^{(i \not\rightarrow j)} + e^{(j \not\rightarrow i)}}{e^{(j \not\rightarrow i)}}}{\binom{e^{(i \rightarrow j)} + e^{(j \rightarrow i)} e^{(i \not\rightarrow j)} + e^{(j \not\rightarrow i)}}{e^{(j \rightarrow i)} + e^{(j \not\rightarrow i)}}} \equiv \\
&\equiv \frac{(e^{(i \rightarrow j)} + e^{(j \rightarrow i)})! (e^{(i \not\rightarrow j)} + e^{(j \not\rightarrow i)})! (e^{(i \rightarrow j)} + e^{(i \not\rightarrow j)})! (e^{(j \rightarrow i)} + e^{(j \not\rightarrow i)})!}{e^{(i \rightarrow j)}! e^{(j \rightarrow i)}! e^{(i \not\rightarrow j)}! e^{(j \not\rightarrow i)}! (e^{(i \rightarrow j)} + e^{(j \rightarrow i)} + e^{(i \not\rightarrow j)} + e^{(j \not\rightarrow i)})!}.
\end{aligned} \tag{7}$$

The relations $i-j$, i.e., the time windows, whose p -values lie under the criterion of level of significance $\alpha = 0.05$ (i.e., $p \leq C_\alpha$) were rejected.

For the rest of relations $i-j$, the *probabilities of following* were then defined using the sums of significant evidences written in Eqs. 3–6. As an example can be shown

$$P^{(i \rightarrow j)} = \frac{e^{(i \rightarrow j)}}{e^{(i \rightarrow j)} + e^{(i \not\rightarrow j)}} = \left[1 + \frac{e^{(i \not\rightarrow j)}}{e^{(i \rightarrow j)}} \right]^{-1}, \tag{8}$$

where $P^{(i \rightarrow j)}$ is a chance that object i follows object j . The advantage of the proposed measure of following is not only its clear meaning but also the fact that it decoupled from direct measurements: first its transformation to correlation space, and then from correlation space to probability space. Thus, it allowing comparison and general analysis of very different systems, because even absolute values of correlation are not matters, only their combinations and ratios. The obtained following matrix is of the size $n_{obj} \times n_{obj}$ in case of n_{obj} objects and is typically sparse, thus it is natural to convert it to a directed graph (treating the following matrix as an adjacency matrix). The orientation of the network edges follows the comparison of the values of probabilities $P^{(i \rightarrow j)}$ and $P^{(j \rightarrow i)}$. Examples of such graphs (visualized in a way that a higher probability of following corresponds to a shorter edge) are shown in Figure 4A. These graphs are defined at each recorded time (Video in Supporting files) and have a very clear behaviouristic meaning, showing who follows whom.

The approach described above utilizes only a single parameter – a size of the time window L . The obtained network is thus a function only of the time t and the parameter L .

Biological relevance

In order to verify the method, we conducted a very simple experiment: the fish were freely swimming in a aquarium for 15 min. The experiment was repeated 10 times in the same time of different days to investigate the stability of the fish school and repeatability of measurements. An output of the method is a directed graph defined for each time frame (Video in Supporting files). Interpretation of these graphs is straightforward: the nodes correspond to the observed objects (fish individuals in our case), length of the edges inversely reflect the probability of following (the shorter the edge, the higher the chance of following). The arrows show who follows whom.

In order to show the variability of the network of following over time, we partition the graphs adjacency matrices into two groups by k -means. The networks of following dominating in each of the groups are shown in Figure 4A. Of course, the real situation is more complicated and two groups of the networks of following is only the minimal illustrative example. The networks in Figure 4A are very similar, almost the same, but directions of edges are changed to the opposite and fish #1 and #6 simply swapped their positions. Fish #3 has the most prominent set of features among all. Fish #3 is situated in the center and has a quite strong connectivity to all other fish and changed its role in the school completely (depicted by a reverse direction of the network edges). Even without biological analysis one can assess that this fish is somehow important. Fish #2 is also connected to everyone, but the connections are weak (the lengths of network edges are relatively long). Fish #5 and #6 changed their mutual distances and did not show any distinct feature.

To quantify the intensity of the relations among the fish, two centrality measures – in-degree and out-degree – were calculated for each node. The in/out-degree parameter is characterized as number of edges entering/emerging from a network node in a time window. After that, for all ten experiments a probability density function for values of in/out-degree parameters was estimated by the kernel density estimation (Figure 4B). The obtained distribution is nor unimodal, nor trivial. To switch to a parametric statistics, a mixture of 4 Gaussians was fitted to this distribution (Figure 4B). In- and out-degree parameters each can be then described by 12 essential parameters: 4 sets of [component proportion, mean value, variance], each of them corresponding to one peak in the distribution.

The clearest interpretation of the results provide component (peak area) proportions in the probability density functions (compared with mean values or variances) – this approach is closely related to frequency analysis. A higher value of the component proportion corresponds to a longer time spent in the relevant mean value (the components are sorted in ascending order according to the mean values). A robust measure of in/out-degree due to a relatively low frequency of occurrence is a sum of the 3rd and the 4th component proportion, showing how frequently the fish exhibits a high in/out-degree state. The box plot of in-degree states for all 6 fish from 10 experiments is depicted in Figure 4C. Fish #3 and #4 show the highest in-degree state. These individuals are frequently followed and literally *lead* the school. However, #3 has a low out-degree (rarely following someone) and #4 has a high out-degree. We interpret this as meaning that fish #3 is a leader and fish #4 can be called a coordinator. The issue is that there is no clear definition of possible roles, only consensus that they exist¹³. This is supported by the plots in Figure 4A. The role of the *coordinator* changes diametrically (the coordinator can be followed or following). In general, such a network shows an oscillatory process over time and is not trivial (it is not possible to obtain from one cluster another one only by a simple changing the direction of edges). We have not investigated this phenomenon deeper yet but a similar oscillation process has been already observed before¹⁴. The mean value, which corresponds to the out-degree Gaussian components 3 and 4 for fish #1, is significantly lower than the average (Figure 4D). The combination with a very low in-degree component proportion may support the hypothesis that fish #1 is *oppressed* or, more precisely, *unsocial*. Fish #1 is never a leader but also does not follow the school too much.

Thus, even the most simple analysis of the obtained graphs gives an insight into the school structure, which is consistent between experiments. Of course, the detected candidates for *roles* have to be rigorously tested on different schools and even on different species. Although the complexity of the observed phenomena is quantifiable. Our results are in agreement with the trend recently published in research papers^{13,15,16} that variability in individual behaviour matters in collective behaviour. We think that this variability is not only important, but also essential for explanation of the observed phenomena. However, further studies will be needed, including a detailed comparison of the obtained graphical results with visual observations.

3 DISCUSSION AND CONCLUSIONS

The approach to collective movement quantification proposed in this paper is both informative and easy to interpret. It can be applied to any kind of multiple trajectory data, irrelevant to the species, level or even type of organization (it can be used for flocks of drones or military ships). The approach has only one adjustable parameter – the time window selected according to the system type. Or, one can consider a spectrum of networks for all windows. This makes the method effectively model-free. Although, the method seems to be not too general. The interpretation of the obtained graphs is always up to the researcher. We will investigate much deeper the possible roles in these graphical networks and their agreement with *a priori* biological meaning.

Even a limited application such as a single group of a single species showed an interesting result: the observed roles in the school are not demonstrated all the time, but rather for a time of necessity. This addresses a pitfall of many psychological approaches, which assign a single personality type (temperament or MBTI model¹⁷) to an agent unambiguously and then predict interactions based on this assignment. But it does not work in this way and we can clearly see why: even very simple species have flexible roles. It is more correct to speak about a distribution of such assignments (attributes, categories), or, rather, conditional distributions of the roles, which are dependent on a given situation.

The main advantage of this method, however, is not a generality, but its applicability. It allows to convert widespread, well-known tracking data to the time dependent graphs (sometimes called coevolution networks^{18,19}), which are one of the hottest topics of modern data mining²⁰ and collective behaviour analysis²¹. We expect that this method will benefit all parties – biologists and data scientists – and allows the researchers to convert ethological assumptions and subjective observations to physical quantities.

Code availability

The Matlab code is available in supplementary materials under the MIT license.

Supporting files

Video. Time changes of the networks of following (i.e., fish school configurations) during the experiment (video). Top view (*upper left*), bottom view (*upper right*), front view (*lower left*) of fish school in the aquarium, and network of following (*lower right*).

Author contributions statement

KL collected the image data; he is the developer of the algorithm and the main author of the paper. RR proofread the paper and contributed critically to the results. DŠ is the group leader responsible for funding the research and the inventor of the aquarium device.

Competing interests

All authors declare no conflict of interests.

Funding

This work was supported by the Ministry of Education, Youth and Sports of the Czech Republic—projects CENAKVA (LM2018099) and from the European Regional Development Fund in frame of the project Image Headstart (ATCZ215) in the Interreg V-A Austria–Czech Republic programme. The work was further financed by the project GAJU 017/2016/Z.

4 METHODS AND MATERIALS

Fish breeding

As a model organism we used a Tiger Barb (*Puntigrus tetrazona*) in a group of 6 individuals.

Between the experiments, the fish lived in a relatively large home aquarium ($60 \times 35 \times 40$ cm 3). The aquarium was disinfected with ethanol, boiling, and sodium hydrogen carbonate. The home aquarium was designed as a simulation of the natural environment with involved aquatic plants and stones (4–8 mm). The fish were kept at a 12/12 artificial daylight cycle and 25 °C. The aquarium was illuminated by a Sera LED 360 (20 V, 8.1 W; Heinsberg, Germany). The parameters of water were temporarily adjusted according to the conditions prevailing in the aquarium: the concentration of ions Mg $^{2+}$, Ca $^{2+}$, and NO $^{3-}$ was adjusted to 4.9, 12.0, and 5.5 mg·L $^{-1}$, respectively; pH 6.9; hardness 2.8 °H. The aquarium was equipped with an air pump Sera Air 110 (Heinsberg, Germany), water heater with thermostat and thermometer. Water circulation was ensured by a

separate filter Sera Fil Bioactive 130 L (Heinsberg, Germany). The validation test of water quality was performed at weekly intervals and before each experiment, at the same time the condition of the fish is assessed. The fish were fed (predominately fed by Tetra Min, Tetra, Melle, Germany) once a day (at 7 a.m.), 1 h after turning the aquarium illumination on.

Image data collection

The experiments were conducted at (11 ± 0.5) a.m. on 10 consecutive days (including the weekend). The experimental set-up is shown in Figure 1. The small ($38.5 \times 20 \times 14$ cm 3 , maximal volume 8-L; 6-L used) aquarium was located inside a LED box, which provided homogeneous illumination from all angles. Water in the aquarium came from the home aquarium; water quality was validated before each experiment. Along 4 sides of the aquarium, mirrors were located. But only two of the mirrors were used – above and below the aquarium – which allowed us simultaneous observations of the aquarium from 3 sides (one side directly and two sides in mirrors). The fish were transported to the small aquarium under full illumination 5 min before each experiment. Of course, such a set-up may cause significant stress to the fish. However, the preliminary exposure the fish to light significantly mitigated the behaviour alteration. Moreover, this species particularly has a keen intellect and good memory, thus the experimental conditions are not new every day and the stress is alleviated. Above all, the aim was not to fully eliminate the stress, but make it repeatable and systematic (each individual fish perceives the stress in the same way. All experiments were conducted with a single group of fish in order to eliminate inter-group variability. It is not yet known, how different school structure can be (even for the same species and group size).

To reduce the number of errors in identifying individual fish, data was collected by a 12-bit Ximea MX124CG-SU-X2G2-FAB rgb camera with a scanning frequency of 0.4 Hz and high resolution in the experimental aquarium during the experiment. The size of the fish in the digital image corresponded to approx. 50×30 px ($5 \mu\text{m}^2 \cdot \text{px}^{-1}$).

ABBREVIATIONS AND SYMBOLS

A_i, A_j	position (scalar) of the first object in two consecutive time windows i and j , respectively (in our specific case $A \equiv X_i$)
B_i, B_j	position (scalar) of the second object in two consecutive time windows i and j , respectively (in our specific case $B \equiv X_j$)
\vec{A}_i, \vec{A}_j	vector position of the first agent in frames i and j , respectively (in our specific case $\vec{A} \equiv \vec{X}_i$); $\vec{A}_i = (x_{Ai}, y_{Ai}, z_{Ai})$ and $\vec{A}_j = (x_{Aj}, y_{Aj}, z_{Aj})$ in the 3D Euclidian space
\vec{B}_i, \vec{B}_j	vector position of the second agent in frames i and j , respectively (in our specific case $\vec{B} \equiv \vec{X}_j$); $\vec{B}_i = (x_{Bi}, y_{Bi}, z_{Bi})$ and $\vec{B}_j = (x_{Bj}, y_{Bj}, z_{Bj})$ in the 3D Euclidian space
C_α	α -dependent criterion of the Fisher test
CNN	convolutional neural network

D_{ij}	difference between the scalar distances in two consecutive time frames i and j
e	frequency of occurrence of significant evidences in the experiment
\mathbf{F}	agent's future state (location)
\mathbf{FF}	follower's and leader's future states correlate (neutral hypothesis)
\mathbf{FN}	follower's future state correlates with leader's current state (supporting hypothesis)
\mathbf{FP}	follower's future state correlates with leader's past state (supporting hypothesis)
i, j	labels of agents (fish)
i, j	labels of two consecutive time windows in the image sequences; $i, j \in \mathbb{N}$
$i \rightarrow j$	agent i follows agent j
$i \not\rightarrow j$	agent i follows agent j
$j \rightarrow i$	agent j follows agent i
$j \not\rightarrow i$	agent j follows agent i
k	number of clusters in k -means analysis
KDE	kernel density function
L	size of the time window
n	element of the set N
n_{obj}	number of agents in the experiment; $n_{obj} = 6$ fish
N	set of combinations of time windows having no relation to the hypothesis that one object follows another one; $N = \{\mathbf{PP}, \mathbf{NN}, \mathbf{FF}\}$
\mathbf{N}	number of time windows in the sequences
\mathbf{N}	agent's current state (location)
\mathbf{NF}	follower's current state correlates with leader's future state (rejecting hypothesis)
\mathbf{NN}	follower's and leader's current states correlate (neutral hypothesis)
\mathbf{NP}	follower's current state correlates with leader's past state (supporting hypothesis)
p	p -criterion of the Fisher exact test
P	probability of following that one agent follows another
\mathbf{P}	agent's past state (location)
\mathbf{PF}	follower's past state correlates with leader's future state (rejecting hypothesis)
\mathbf{PN}	follower's past state correlates with leader's current state (rejecting hypothesis)
\mathbf{PP}	follower's and leader's past states correlate (neutral hypothesis)
r	element of the set R
R	set of combinations of time windows rejecting the hypothesis that one object follows another one; $R = \{\mathbf{PN}, \mathbf{PF}, \mathbf{NF}\}$
s	element of the set S
S	set of combinations of time windows supporting the hypothesis that one object follows another one; $S = \{\mathbf{NP}, \mathbf{FP}, \mathbf{FN}\}$
t	time; the center of the time window
VGG	Visual Geometry Group (at the Oxford University)
α	level of statistical significance

REFERENCES

1. Bak-Coleman, J. B. *et al.* Stewardship of global collective behavior. *Proceedings of the National Academy of Sciences* **118**, e2025764118 (2021).
2. Gibbs, K. A., Urbanowski, M. L. & Greenberg, E. P. Genetic determinants of self identity and social recognition in bacteria. *Science* **321**, 256–259 (2008).
3. Vicsek, T. & Zafeiris, A. Collective motion. *Physics Reports* **517**, 71–140 (2012).
4. Warren, W. H. Collective motion in human crowds. *Current Directions in Psychological Science* **27**, 232–240 (2018).
5. Romero-Ferrero, F., Bergomi, M. G., Hinz, R. C., Heras, F. J. H. & de Polavieja, G. G. id-tracker.ai: tracking all individuals in small or large collectives of unmarked animals. *Nature Methods* **16**, 179–182 (2019).
6. de Vries, H. An improved test of linearity in dominance hierarchies containing unknown or tied relationships. *Animal Behaviour* **50**, 1375–1389 (1995).
7. Perez-Escudero, A., Vicente-Page, J., Hinz, R. C., Arganda, S. & de Polavieja, G. G. id-Tracker: tracking individuals in a group by automatic identification of unmarked animals. *Nature Methods* **11**, 743–748 (2014).
8. Liu, S. & Deng, W. Very deep convolutional neural network based image classification using small training sample size. In *2015 3rd IAPR Asian Conference on Pattern Recognition (ACPR)*, 730–734 (IEEE, 2015).
9. Lonhus, K., Štys, D., Saberioon, M. & Rychtáriková, R. Segmentation of laterally symmetric overlapping objects: application to images of collective animal behavior. *Symmetry* **11**, 866 (2019).
10. Székely, G. J., Rizzo, M. L. & Bakirov, N. K. Measuring and testing dependence by correlation of distances. *The Annals of Statistics* **35**, 2769–2794 (2007).
11. Székely, G. J. & Rizzo, M. L. Brownian distance covariance. *The Annals of Applied Statistics* **3**, 1236–1265 (2009).
12. Fisher, R. A. On the interpretation of χ^2 from contingency tables, and the calculation of P . *Journal of the Royal Statistical Society* **85**, 87 (1922).
13. Marras, S. & Domenici, P. Schooling fish under attack are not all equal: some lead, others follow. *PLoS ONE* **8**, e65784 (2013).
14. Swain, D. T., Couzin, I. D. & Leonard, N. E. Coordinated speed oscillations in schooling killifish enrich social communication. *Journal of Nonlinear Science* **25**, 1077–1109 (2015).

15. del Mar Delgado, M. *et al.* The importance of individual variation in the dynamics of animal collective movements. *Philosophical Transactions of the Royal Society B: Biological Sciences* **373**, 20170008 (2018).
16. Shaw, A. K. Causes and consequences of individual variation in animal movement. *Movement Ecology* **8**, 12 (2020).
17. Briggs-Myers, I. & Briggs-Myers, P. *Gifts Differing* (John Murray Press, 1995).
18. Farajtabar, M. *et al.* COEVOLVE : A Joint Point Process Model for Information Diffusion and Network Evolution. *Journal of Machine Learning Research* **18**, 49 (2017).
19. Wang, W., Liu, Q.-H., Liang, J., Hu, Y. & Zhou, T. Coevolution spreading in complex networks. *Physics Reports* **820**, 1–51 (2019).
20. Liu, X. F., Chen, H.-J. & Sun, W.-J. Adaptive topological coevolution of interdependent networks: Scientific collaboration-citation networks as an example. *Physica A: Statistical Mechanics and its Applications* **564**, 125518 (2021).
21. Davidson, J. D., Vishwakarma, M. & Smith, M. L. Hierarchical approach for comparing collective behavior across scales: cellular systems to honey bee colonies. *Frontiers in Ecology and Evolution* **9**, 581222 (2021).

Table 1: The Fisher test contingency table for verification of the hypothesis of measure of following.

Following	Object i	Object j	Total rows
Not following	$e^{(i \rightarrow j)}$	$e^{(j \rightarrow i)}$	$e^{(i \rightarrow j)} + e^{(j \rightarrow i)}$
	$e^{(i \not\rightarrow j)}$	$e^{(j \not\rightarrow i)}$	$e^{(i \not\rightarrow j)} + e^{(j \not\rightarrow i)}$
Total columns	$e^{(i \rightarrow j)} + e^{(i \not\rightarrow j)}$	$e^{(j \rightarrow i)} + e^{(j \not\rightarrow i)}$	$e^{(i \rightarrow j)} + e^{(i \not\rightarrow j)} + e^{(j \rightarrow i)} + e^{(j \not\rightarrow i)}$

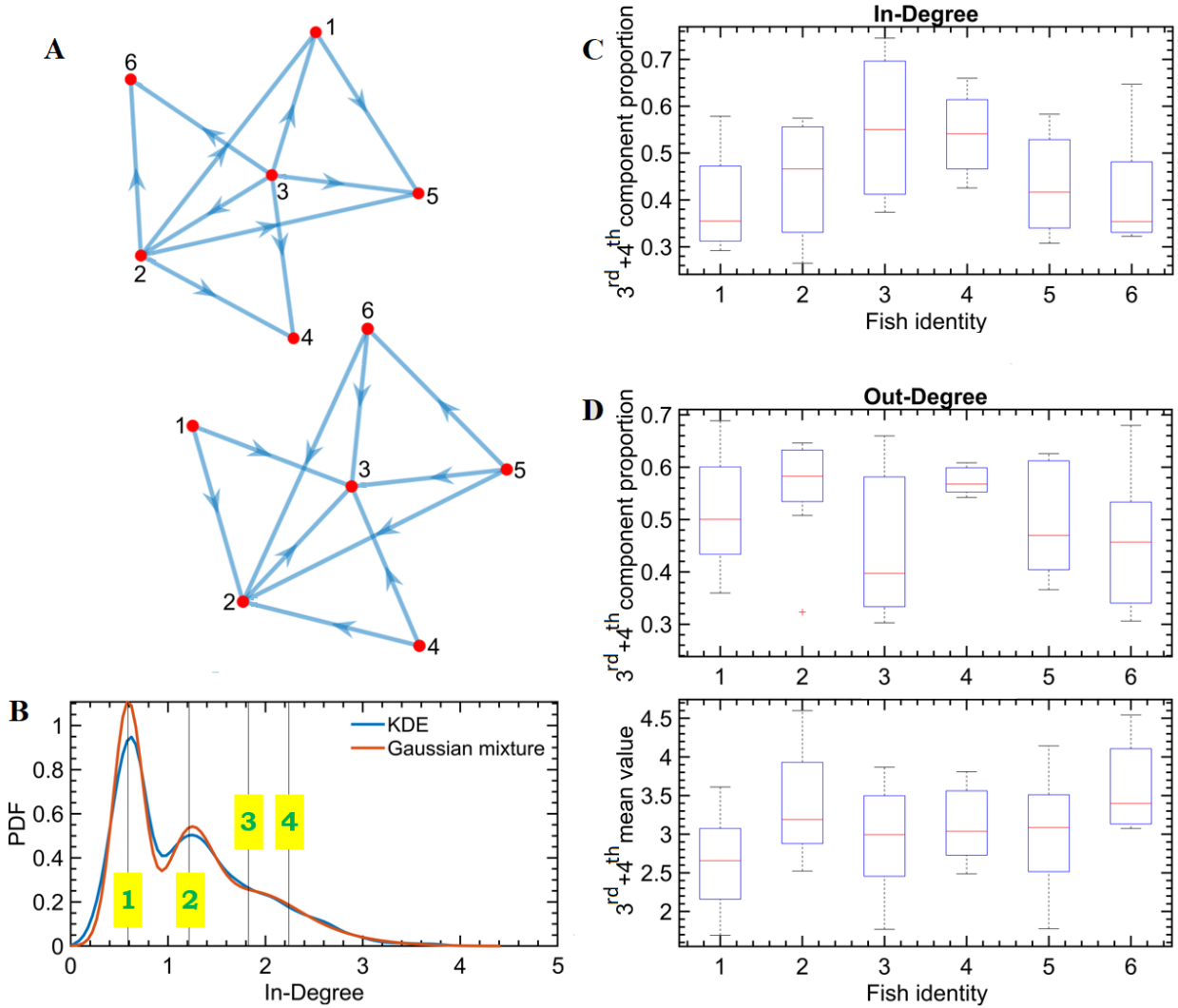


Figure 4: (A) Two typical networks of following in a school of 6 fish. (B) The kernel density estimation (KDE) and the Gaussian fitting for the in-degree parameter of the network of following. For out-degree parameter the distributions are analogous to the in-degree parameter. (C) The distribution of intra-experiment in-degree Gaussian fitting component proportions. (D) The distribution of intra-experiment out-degree Gaussian fitting component proportions and mean values.